

## MECHANICAL AND MICROSTRUCTURE PROPERTIES OF HIGH POROSITY SINTERED Ti-6Al-4V POWDER FOR BIOMEDICAL APPLICATIONS

---

**Montasser Dewidar**<sup>1,2</sup>

<sup>1</sup> Department of Mechanical Design and Materials, High Institute of Energy, South Valley University Aswan, Egypt.

<sup>2</sup> Material & Fracture Lab., Department of Mechanical Design, Chonbuk National University, Duckjin 1-664-14, Jeonju, JB561-756, South Korea.  
[Dewidar5@hotmail.com](mailto:Dewidar5@hotmail.com)

(Received August 2, 2006 Accepted September 23, 2006)

**ABSTRACT** – Bone injuries and failures often require the inception of implant biomaterial. Recently, research in this area has received increasing attention. Particularly, porous metals are attractive due to its unique physical, mechanical, and new bone tissue ingrowth properties. In the present study, the production of highly porous Ti-6Al-4V parts by powder metallurgical technology is described. A space-holder method used carbamide with different particle size to produce parts with porosities between 35% to 70%. Spherical pores with size ranged from 560  $\mu\text{m}$  to 1.0 mm were obtained depending on the size distribution of the space holder. The compressive strength and Young's modulus of porous Ti-6Al-4V were determined. Results indicated that compressive strength and Young's modulus decrease with increasing porosity and pore size. The porous parts are examined using scanning electron microscopy. The microstructure of porous materials is presented, aiming preferentially at biomedical applications. The results show that this process is promising to fabricate biomaterials for bone implants.

**KEYWORDS:** Ti-6Al-4V; Porous material; Powder metallurgy; Space-holder; Mechanical properties

### 1. INTRODUCTION

Bone injuries and failures often require the inception of implant biomaterials. Recently, research in this area has received increasing attention. Various artificial implant biomaterials, such as metals, polymeric materials and ceramics are being explored to replace diseased bones [1-3].

Metals and alloys are widely used as implant biomaterials. Among these metallic biomaterials, titanium and its alloys which have an excellent combinations of structural and mechanical properties such as high strength to weight ratio, good corrosion resistance and superior biocompatibility with the surrounding tissue [4]. The main problem concerning metallic implants in orthopedic surgery is the mismatching

between the modulus of elasticity of metallic titanium implant (110 GPa) and the modulus of elasticity of bone (10-30 GPa) [5-7]. The strength and modulus of elasticity of the titanium and its alloys can be controlled using porous material with different porosity to match the strength and the modulus of elasticity of the natural bone. The low elastic moduli of porous titanium alloys are expected to reduce the amount of stress-shielding at the bone where the metallic part is implanted. This stress-shielding leads to bone resorption and then eventual loosening of the implant, and hence to prolong implant life time [8]. In addition, by increasing the match of the strength and the modulus of elasticity between the bone and titanium alloys, it is expected to result in better performance of the implant bone compound.

Many available methods for producing porous titanium and titanium alloy include sintering together of the particles [9] or plasma spraying of the powder on a dense substrate followed by the cutting of the porous layer [10], solid-state foaming by expansion of argon-filled pores [11-13] and polymeric sponge replication [14]. However, none of these conventional techniques has allowed for building parts with a completely controlled size and shape of the pore. The porous matrix must be designed to satisfy many requirements such as; the porous structure must be designed with high porosity to provide sufficient space for attachment of the new bone tissues and transport of the body fluids, the structure must be interpenetrated to allow the ingrowths of cells vascularization and diffusion of body, and the material must be of appropriate mechanical properties to resist handling during implantation and in vivo loading.

The imperfection of the conventional techniques has encouraged the use of space-holder technique. This technique depends on mixing of the metallic powder with space holder, which can be removed without contaminating of the titanium powders [15]. All details about this technique can be found elsewhere [15].

This work was undertaken to develop a high porous Ti-6Al-4V parts with controllable porosity, pore size, and pore shape. A new fabrication technique, which includes the adding of space holder into the powder to manufacture high porous Ti-6Al-4V was investigated. Shrinkage during sintering was investigated. The compression tests were performed on the porous Ti-6Al-4V samples for studying the mechanical properties. The modulus of elasticity of the samples was determined. The fabricated parts were examined and characterized by scanning electron microscopy.

## 2. EXPERIMENTAL PROCEDURE

Ti-6Al-4V powder with average size of 56  $\mu\text{m}$  (supplied by SE-JONG Materials Ltd. Korea) was used in the present experimental work. The morphology of Ti-6Al-4V powder and carbamide (space holder) particles were examined by scanning electron microscope (SEM) and digital camera respectively as shown in **Fig. 1 a** and **b**. From **Fig. 1 (a)**, it can be seen that the majority of the Ti-6Al-4V powders are irregular with a mean diameter of 56  $\mu\text{m}$ . The chemical composition of Ti-6Al-4V is given in Table 1. Spherical carbamide with different particle diameters (0.56, 0.8, and 1mm) was used as the present space holder. Lide [16] reported that carbamide consider as a candidate material for pore forming additive. The selection of carbamide as space-holder material

is based mainly on its ability to decompose completely at low temperature avoiding the reaction with the host powder without any excessive contamination for the Ti-6Al-4V powder. In addition, there is no risk of Ti-6Al-4V deterioration.

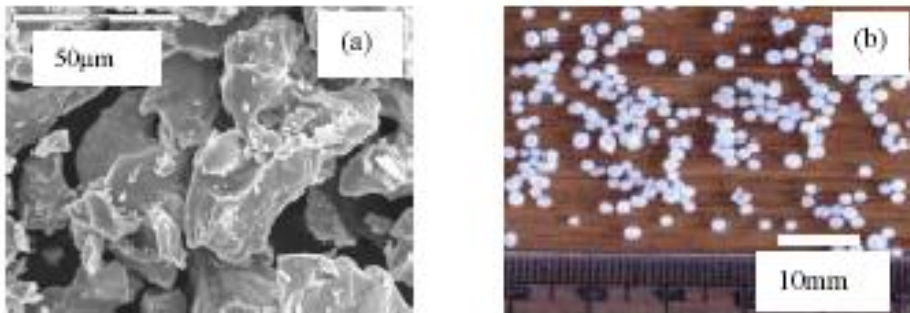


**Fig. 1.** Morphology of initial powders, (a) Ti-6Al-4V powders, and (b) carbamide particles.

**Table 1:** Chemical composition of Ti-6Al-4V powder.

Ti	Si	Fe	C	H	N	O	V	Al	Element
Bal.	0.04	0.27	0.013	0.003	0.007	0.17	3.93	6.38	(wt %)

The weight ratios of the Ti-6Al-4V powder to the amount of space holder were calculated to obtain defined porosities of 25, 50, and 70% in the sintered compact samples. The Ti-6Al-4V powders were mixed thoroughly with carbamide particles in a rolling container for an hour. To prevent the dissimilar powder from segregation a small amount of ethanol was sprinkled during blending. The powder particles adhered to the surface of the space holder. All the samples used in the present investigation were fabricated by cold compaction using a manually operated uniaxial press. A wide range of compaction pressures was used to obtain different specimen densities. The mixture was uniaxially pressed at 250, 350, 450, and 550 MPa into cylindrical compacts with diameter  $d=12$  mm. The height of the cylindrical samples after pressing was approximately 15 mm. The mixing of any additional lubricant is not necessary. This is of special importance for the manufacturing of Ti-4Al-6V parts, where lubricant could be an additional source of impurities in the final product.

The decomposition of carbamide in the green samples was carried out in vacuum at  $200^{\circ}\text{C}$  for 2 hrs to avoid the solid substance burnt  $(\text{NH}_2\text{CO})_2\text{NH}$ , which leads to an unacceptable increasing of impurity of the final products. The compact samples were then sintered under a vacuum of  $2 \times 10^{-3}$  Torr. The sintering process is consisted of two steps; the first step includes holding stage at  $850^{\circ}\text{C}$  for one hour to allow for sample outgassing; surface oxides, water molecules and contaminants volatilize off from the sample surface prior to holding at the sintering temperature. These gasses and oxides must be dissipated before final consolidation in order to prevent the samples distortion. The second step was including holding stage at  $1200^{\circ}\text{C}$  for 2 hrs under vacuum of  $2 \times 10^{-3}$  Torr.

The relative densities of green and sintered specimens were determined based on their weight and size using the theoretical density of corresponding composition. Porosity  $P$  (in percentage of volume) was calculated by measuring the apparent density ( $\rho_b = \text{weight of sample}/\text{volume of sample}$ ) of sample by using the formula:

$$P = \frac{1 - \rho_b}{\rho_s} \times 100 \quad (1)$$

where  $\rho_s$  is the density of 100% dense material. The shrinkage in axial and radial directions was measured. The compression tests were carried out at room temperature with an initial testing speed of 0.5 mm/min. Young's modulus,  $E$  (GPa), was measured using an ultrasonic technique. The ultrasonic technique is ideal for highly porous materials because deformations of the material caused by the ultrasonic energy are sufficiently small such that plasticity can be avoided. A transducer transmitted a sinusoidal signal to the front surface of the specimen and recorded the wave reflected by the opposite surface. The wave velocity was given directly by the delay between emitted and received signal and the sample dimensions. To minimize scattering effects the wavelengths were chosen to be smaller than the dimension of the specimen, but greater than the size of the pores. The Young's modulus calculated using the following relationship [17]:

$$E = \rho \frac{3V_L^2 V_T^2 - 4V_T^4}{V_L^2 - V_T^4} \quad (2)$$

Where  $\rho$  is the density of the material, and  $V_L$  and  $V_T$  are the longitudinal and transverse wave velocity. The microstructure of sintered parts were studied by scanning electron and optical microscopy.

## 2. RESULTS AND DISCUSSION

The procedure which used during this work is basically simple: mixing space-holder with Ti6Al4V powder, cold compaction, then decomposition the space-holder in a relatively low temperature, and finally sintering to obtain the required porous Ti-6Al-4V. The porosity is up to 70% with complete open structure. The increases of relative density of Ti-6Al-4V before sintering and after sintering are shown in **Figure 2**. Generally, they become less with increasing space-holder amount and porosity of compacts before sintering. The percentage of Ti-6Al-4V in the porous is reduced at higher contents of the space-holder. The variation of relative densities before and after sintering of parts with 35%, 50%, and 70% porosity were found to be around 18%, 13% and 10% respectively (see **Figure 2, a, b, and c**). This is due to the preferred shrinkage of micropores within the Ti-6Al-4V framework. Therefore, the decreased volume of Ti-6Al-4V framework reduces the microscopic densification of samples. On the other hand, increasing the compaction pressure leads to increase the relative density of the parts with a small value. In addition, the relative densities of samples after sintering were found to be the same. So, a high compaction pressure is recommended which produce green parts with a high strength for handling and measuring without distortion. But at very high compaction pressure may be the Ti-6Al-4V particles tend to be pressed into the space-holder particles causes the formation of cracks in the particles of space-holder. In addition, there is no significant effect of the size of space-

holder on the relative density of Ti-6Al-4V parts before and after sintering. The effect of sintering temperature on porosity is shown in **Figure 3**. As can be seen from this Figure the sintering temperature effects very slightly the densification of Ti-6Al-4V compacts.

Mainly the shrinkage during sintering occurs due to reduction in size of micropores of the compacts. In contrast, German [18] reported that macropores keep their size or tend to increase. Relationship between axial and radial shrinkage of samples and compaction pressure are shown in **Figure 4**. As can be seen from **Figure 4 a, b, c, and d**, as expected, the axial and radial shrinkage decrease with increasing compaction pressure and, also, with enhancement of compact density. Also, the figure shows that there is no significant change of axial and radial shrinkage as a result of increasing contents of space-holder. Therefore, the axial and radial shrinkage grows with increasing the temperature of sintering from 1200 °C to 1250 °C as can be seen from **Figure 5, a and b**. On the other hand, there is no significant effect of the size of space-holder on the axial and radial shrinkage, i.e., the shrinkage have the same trend. Although the axial and radial shrinkage have the same trend, the radial shrinkage was found to be higher than the axial shrinkage for the same samples at the same conditions. The corresponding decrease of volumetric was ranged between 30% and 23.75% for compaction pressure 250 MPa, and 550 MPa, respectively.

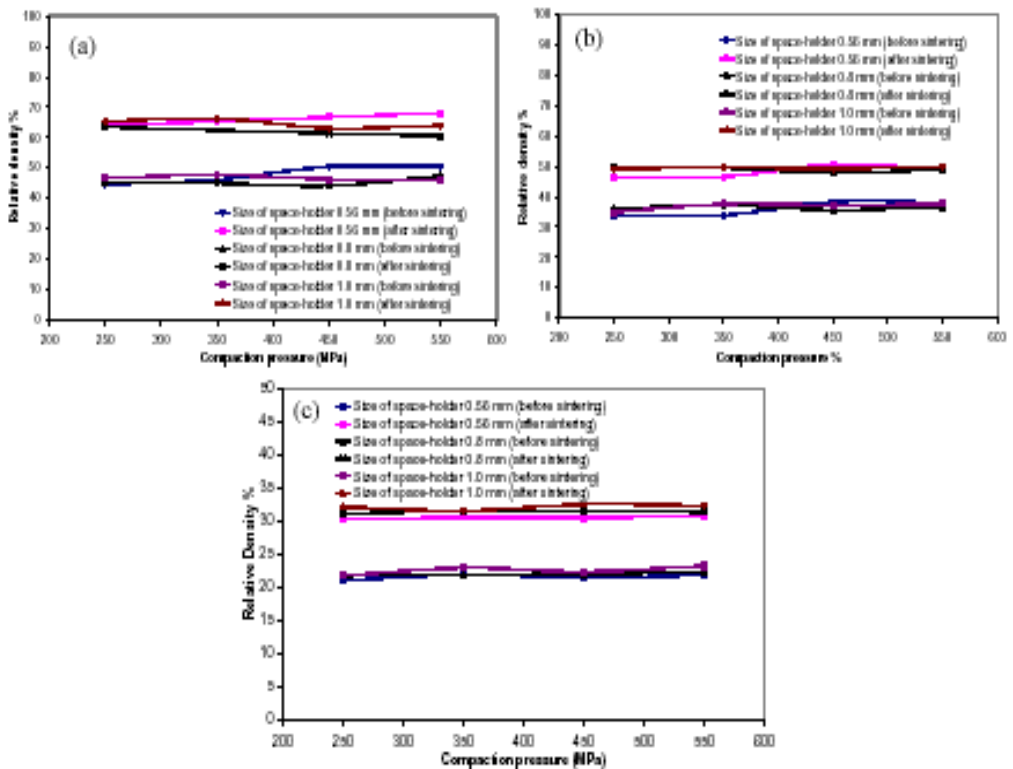


**Figure 2.** Densification of porous parts after sintering at 1200°C for 2h for different volumetric percent, a) 35%, b) 50%, and c) 70 %.

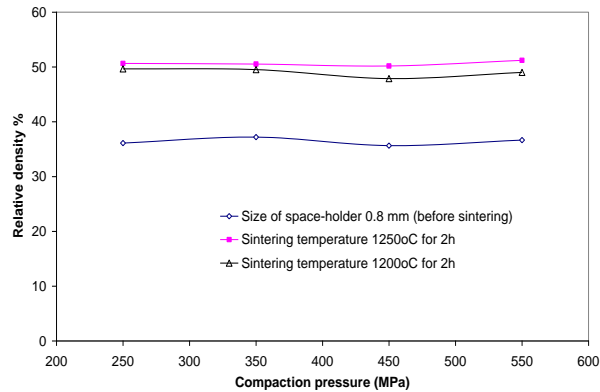


**Figure 3.** Effect of compaction pressure on relative density at different sintering temperature.

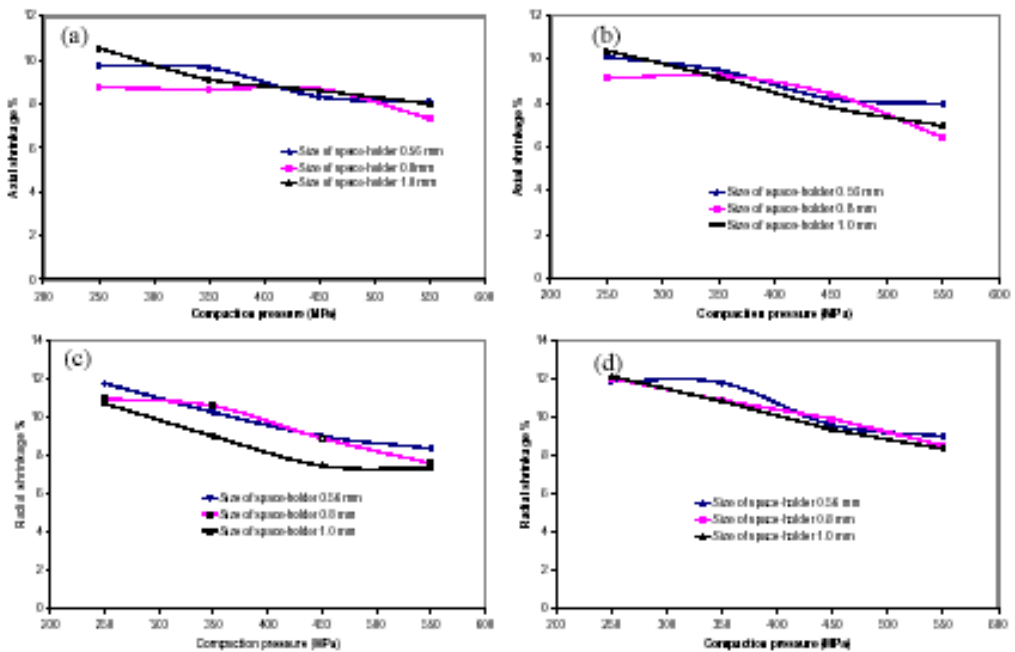


**Figure 4.** Variation of axial shrinkage% and radial shrinkage% effect with compaction pressure for different size of space holder.

The microporosity of the Ti-6Al-4V structure was investigated by scanning electron microscopy. Figure 6 shows the structure of the parts which present two kinds of pores. The first type is micropores with a size of several micrometers, as can be seen in **Figure 6 a**. This type of pores was found between the particles of Ti-6Al-4V resulting from shrinkages that occurred during sintering process. The second type is macropores which arising as a result of space-holder removal (**Figure 6 b, c, and d**). The size of macropores depends mainly on the size of the space-holder ranging from 560  $\mu\text{m}$  to

1.0 mm. The structure of samples pressed with 35, 50, and 70 % of space-holder with size 0.8 mm and sintered at 1200°C for 2h are shown in Figure 6 b, c, and d. It can be seen from this figure that the macropores remain nearly unchanged during the sintering process. In addition the Ti-6Al-4V alloy foams with 70% porosity displayed an interconnected porous structure resembling bone (**Figure 4d**). The lower porosity resulted in less interconnected pores (**Figure 6b**). Obviously, the parts have been a good homogenous of the pores. Also, it can be noticed that some of pores are not of spherical shape. The main reason is that the raw particles of the space-holder have this defect.

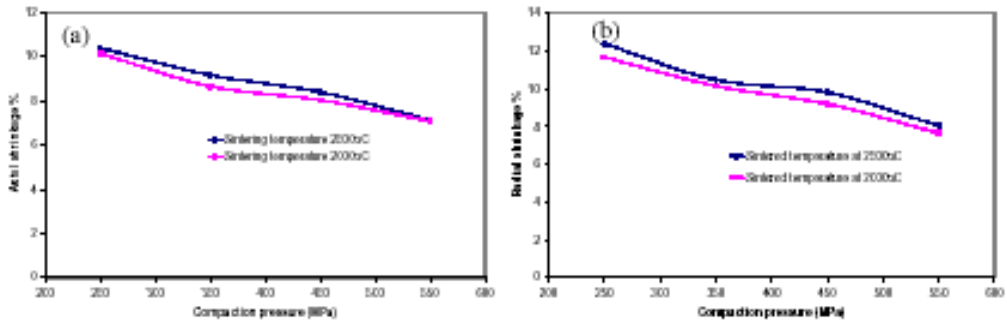


**Figure 5.** Variation of axial shrinkage% and radial shrinkage% effect with compaction pressure for different sintering temperature.

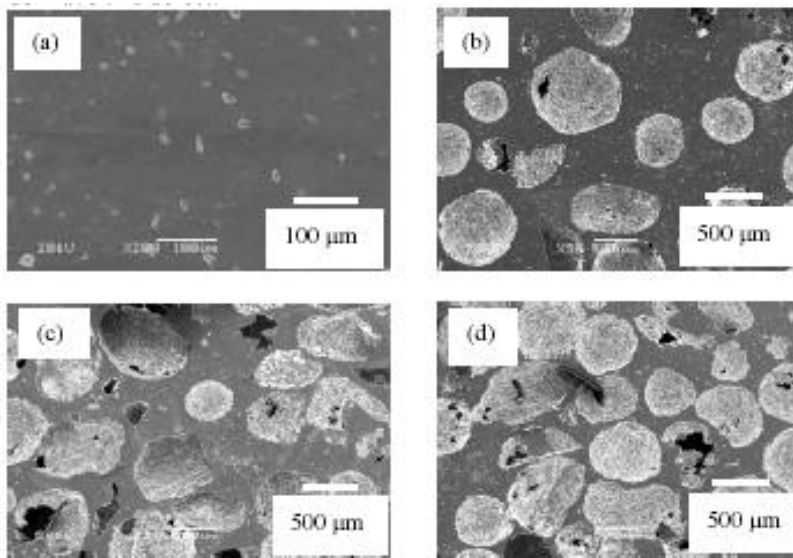


**Figure 6.** SEM micrograph of porous Ti-6Al-4V with 0.8 mm pore size sintered at 1200 °C for 2h in vacuum atmosphere. a) micropores, b) 30% porosity, c) 50% porosity, and d) 70% porosity.

The microstructure of surface of porous Ti-6Al-4V is shown in **Figure 7**. The image in **Figure 7**, (a) indicate clearly the micropores between particles of Ti-6Al-4V.

**Figure 7**, (b) indicates that powder bonding is achieved by neck growth through a solid state diffusion process, and no liquid phase occurs. In addition, the cell walls of porous Ti-6Al-4V part were rough and honeycomb like, as can be seen in **Figure 7 b**. The chemical analysis results of organic residuals (oxygen, carbon, and nitrogen) after the different processing steps are shown in **Figure 8**. It can be seen that the contents of oxygen, carbon and nitrogen remain nearly unchanged after removal of space-holder. After sintering, the concentration of carbon, oxygen, and nitrogen are all increased slightly. The reason for this behavior is probably attributable to residual contaminants in the furnace.

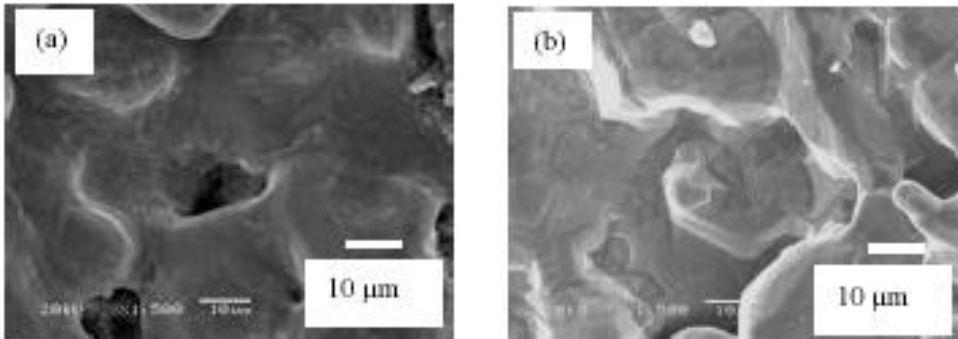


**Figure 7.** Surface of Ti-6Al-4V sample, a) micropores, b) formation of sintering necks.

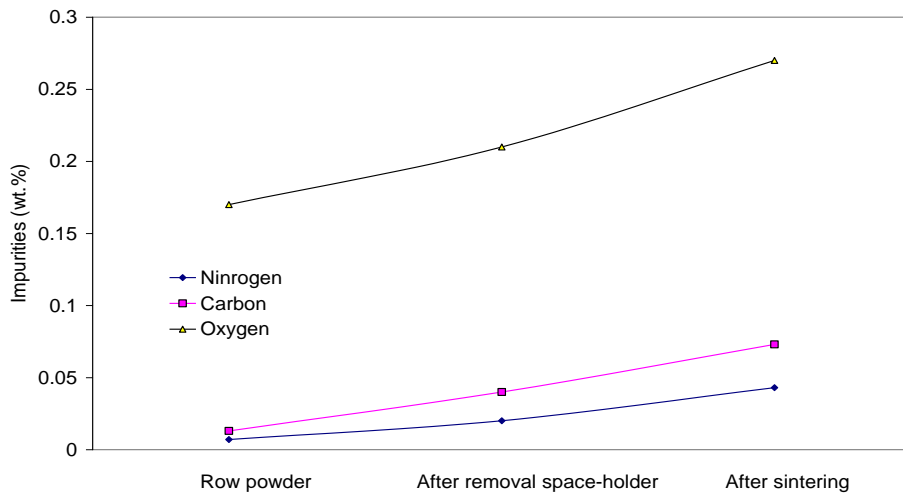


**Figure 8.** Chemical analysis of Oxygen, Carbon and nitrogen contents in Ti-6Al-4V parts after processing steps.

To achieve a functionally satisfying implant in practical applications, porous scaffold design needs to consider both the strength and the Young's modulus. The elastic modulus of bone ranges from 10 to 30 GPa; and the compressive strength ranges from 2 to 200 MPa [19]. To avoid stress shielding the elastic moduli of bone and implants

should be as similar as possible, which may lead to bone resorption and even necrosis. Compressive test was conducted on Ti-6Al-4V parts with a porosity ranged from 35% to 70% to evaluate the mechanical properties. The nominal stress-nominal strain curves for the Ti-6Al-4V sample with pore size 0.8 mm are shown in **Figure 9**. It can be seen that the Ti-6Al-4V foam showed the typical deformation behavior of metallic foams under compressive loading. Generally both the Young's modulus and the peak stress increased with a decrease in porosity. The compressive stress of the Ti-6Al-4V foam with porosity 35%, 50%, and 70% were 400, 225, and 40 MPa respectively. The corresponding Young's modulus were found to be 19, 14, and 11 GPa respectively. The Young's modulus measured by ultrasonic testing is slightly higher than the value which calculated from compressive test. This variation can be explained by localized damage accumulating at very low strain levels in compression testing, in the region where the stress strain curves appear linear, making the material effectively soft. These results confirm the preference for the ultrasonic method to determine elastic properties. It can be seen that the mechanical properties of the foam with porosity 70% were very close to those of the natural bone.

**Figure 10** shows the variations in the stress and Young's modulus of Ti-6Al-4V parts sintered at 1200°C as a function of pore size, where the porosity is 35%. Gibson and Ashby [20] reported that the collapse stress and Young's modulus are not affected by the pore size. But, the results in the present investigation showed that both the peak stress and Young's modulus decreased with an increase in pore size. Miyoshi et al. [21] investigated the mechanical properties of porous aluminum and they revealed that the porous aluminum with the smaller pore size showed higher flow stress than that with the greater pore size. Thus, the experimental results showed that a porous material with a small pore size shows higher flow stress and Young's modulus than that with a large pore size. This may be related to a change in aspect ratio of the wall thickness against the edge length [22].

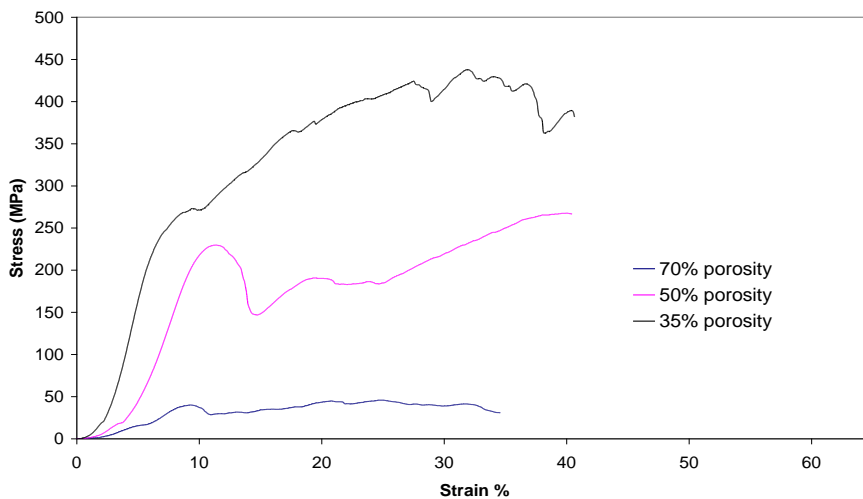


**Figure 9.** Stress-strain curves of porous Ti-6Al-4V parts with various porosities of 35-70%.

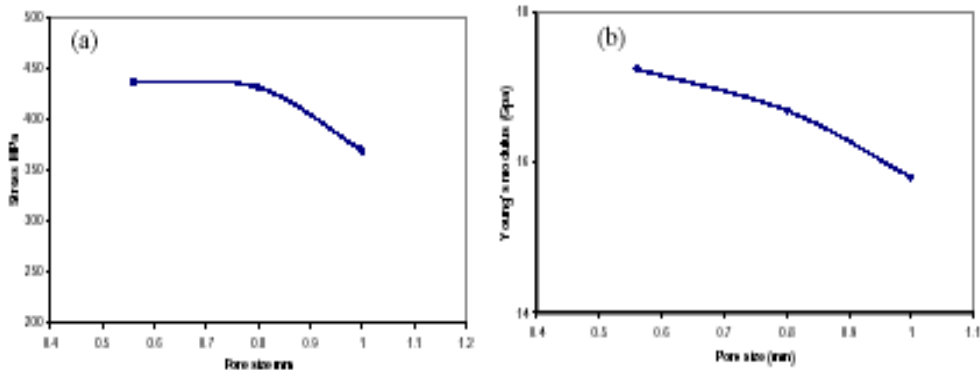


**Figure 10.** Effect of pore size on compressive strength and Young's modulus of Ti-6Al-4V parts sintered at 1200°C for 2h.

#### 4. CONCLUSIONS

Porous Ti-6Al-4V with controlled porosity ranged from 35 and 70%, have been fabricated by a space-holder and powder metallurgy method. Mechanical properties of porous Ti-6Al-4V with the porosity of 35-70% and with the pore size of approximately 560  $\mu\text{m}$  800  $\mu\text{m}$  and 1 mm were investigated by compressive tests focusing on the effects of the porosity and pore size on the strength and Young's modulus. Results indicated that the Young's modulus and compressive stress decreases with an increase in porosity and pore size. The compressive stress of the Ti-6Al-4V foam with porosity 35%, 50%, and 70% were 400, 225, and 40 MPa respectively. The corresponding Young's modulus were found to be 19, 14, and 11 GPa respectively. Shrinkage during sintering occurs mainly due to densification of the Ti-6Al-4V structure. Macropores appearing after removal of the space-holder remain nearly unchanged. Initial titanium powder should have a low impurity content to meet the ISO standard for titanium implants. Control of the oxygen and nitrogen level is an issue of special importance. It is being possible, using this technique, to produce highly porous Ti-6Al-4V fulfilling the ISO standard for biomedical implants. One of the prospective fields of application is the production of surgical implants.

#### 5. REFERENCES

- [1] Katti S. K., Biomaterials in total joint replacement, *Colloids and Surfaces B: Biointerfaces*, Vol. 39, Issue 3, pp. 133-142 2004.
- [2] Ramakrishna S., Mayer J., E. Wintermantel and Leong K. W., "Biomedical applications of polymer-composite materials: a review," *Composites Science and Technology*, Vol. 61, Issue 9, pp. 1189-1224 2001.
- [3] Yoshimitsu O., and Emiko G., "Comparison of metal release from various metallic biomaterials in vitro," *Biomaterials*, Vol. 26, Issue 1, Pages 11-21 2005.
- [4] Long M., Rack H. J., "Titanium alloys in total joint replacement-a materials science perspective," *Biomaterials* Vol. 19, pp. 1621-1639, 1998.
- [5] Hyun, I.k. N. Nomura, Masahashi, N., Hanada, S., "Mechanical properties of porous titanium compacts prepared by powder sintering," *Scripta Materialia* 49, Issue 12, pp. 1197-1202, 2003.

- 
- [6] Wen C. E., Mabuchi M., Yamada Y., Shimojima K., Chino Y., and Asahina T., "Processing of biocompatible porous Ti and Mg," *Scripta Materialia*, Vol. 45, Issue 10, pp.1147-1153, 2001.
- [7] Dewidar M.M., Yoon H.C., and Lim J.K., "Mechanical properties of metals for biomedical applications using powder metallurgy process: A review," *Journal of Metals and Materials*, Vol.12, 3, pp. 193-206, 2006
- [8] Okazaki Y., Nishimura E., Nakada H., and K. Kobayashi, "Surface analysis of Ti-15Zr-4Nb-4Ta alloy after implantation in rat tibia," *Biomaterials*, Vol. 22, Issue 6, pp. 599-607, 2001.
- [9] Dunand D. C., "Processing of Ti Foams," *Advanced Engineering Materials*, vol.6, No. 6, pp. 369-376, 2004.
- [10] Tsui Y. C., Doyle C., and Clyne T. W., "Plasma sprayed hydroxyapatite coatings on titanium substrates Part 1: Mechanical properties and residual stress levels," *Biomaterials*, Vol. 19, Issue 22, 2015-2029, 1998.
- [11] Bram M., Kempmann C., Laptev A., Stöver D., and Weinert K., "Investigations on the machining of sintered titanium foams utilizing face milling and peripheral grinding," *Advanced Engineering Materials* Vol. 5, Issue 6, pp. 441-447, 2003.
- [12] Thieme M., Wieters K.P., Bergner F., Scharnweber D.; Worch H., Ndop J., Kim T. J., and Grill W. , Titanium powder sintering for preparation of a porous functionally graded material destined for orthopaedic implants," *Journal of materials science materials in medicine*, Vol. 12, Issue 3, pp. 225-232, 2001.
- [13] Schuh C., Noël P., and Dunand D. C., "Enhanced densification of metal powders by transformation-mismatch plasticity," *Acta Materialia*, Vol. 48, Issue 8, pp. 1639-1653, 2000.
- [14] Fujita T., Agawa A., Ouchi C., and Tajima H., "Microstructure and properties of titanium alloy produced in the newly developed blended elemental powder metallurgy process," *Materials Science and Engineering A*, Vol. 213, Issues 1-2, pp. 148-153, 1996.
- [15] Dewidar M. M., Seo D. W., and Lim J. K., "Processing of High Porosity Ti-6Al-4V by Powder Sintering Process for Biomedical Applications," *Proceeding of Fracture mechanics and application China*, pp. 177-183, 2005.
- [16] D. R. Lide, "CRC handbook of chemistry and physics," 74<sup>th</sup> edn, 4-37; Boca Raton, CRC press Inc. 1994.
- [17] Kikuchi M., Takahashi M., Okuno O., "Elastic moduli of cast Ti-Au, Ti-Ag, and Ti-Cu alloys," *Dental Materials*, Vol. 22, Issue 7, pp. 641-646, 2006.
- [18] R. M. German, "Sintering Theory and Practice," New York, NY, John Wiley & Sons, Inc. 1996.
- [19] Garrett R., Abhay P., and Dimitrios P. A., "Fabrication methods of porous metals for use in orthopaedic applications," *Biomaterials*, Vol. 27, Issue 13, pp. 2651-2670, 2006.
- [20] Gibson J. K., "The mechanical behaviour of cancellous bone," *J Biomech* 18: 317-328, 1985
- [21] Miyoshi T., Itoh M., Akiyama S., and Kitahara A., "Aluminum Foam: Production Process, Properties, and Applications" *Advanced engineering materials*, Vol. 2, Issue 4, pp. 179-183, 2000.

- [22] Nieh T., Kinney J., Wadsworth J., and Ladd A., "Morphology and elastic properties of aluminum foams produced by a casting technique," Scripta Materialia, Vol. 38, Issue 10, pp. 1487-1494, 1998.

## الخواص الميكانيكية والتركييب البنائي للأجزاء ذات المسامية العالية والمصنعة بطريقة التلبيد لمسحوق سبيكة التيتانيوم وذلك لاستخدامها في التطبيقات الطبية

د منتصر دويدار

قسم هندسة التصميم والمواد, المعهد العالي للطاقة, جامعة جنوب الوادي, أسوان. مصر

عادة ما يتطلب غرس أجزاء بديله من العظام الطبيعية في حالة إصابتها أو فشلها في أداء وظيفتها, وفي الآونة الأخيرة فإن البحث في هذا المجال قد جذب الكثير من الاهتمام, خاصة المعادن المصنعة بمسامية عالية وذلك نتيجة لخواصها الطبيعية والميكانيكية الجيدة وكذلك سماحها لنمو الأنسجة الحية خلالها.

في هذه الدراسة تم وصف طريقة إنتاج أجزاء عالية المسامية من سبيكة التيتانيوم بطريقة متالورجيا المساحيق, وقد تم استخدام حافظ للفراغات لتخليق المسام من مادة اليوريا بحجم حبيبات مختلفة لتصنيع أجزاء بنسب مسامية تتراوح ما بين 35 إلى 70% وقد أمكن تخليق مسام بحجم يتراوح ما بين 0.56 مم إلى 1.0 مم اعتمادا على حجم حبيبات اليوريا المستخدمة.

وفي هذه الدراسة تم أيضا تحديد أقصى إجهاد ضغط للعينات وكذلك معامل المرونة وقد أوضحت النتائج أن هاذين العاملين ينقصان مع زيادة نسبة المسامية وكذلك زيادة حجم المسام نفسها, وقد تم فحص العينات باستخدام الميكروسكوب الإلكتروني الماسح.